

GEM: Geometric Entropy Mixing for Optimal LLM Data Curation

Yue Min^{*12} Ziyun Qiao^{*13} Ruining Chen⁴ Yujun Li¹

Abstract

LLM pre-training efficacy increasingly depends on data composition rather than sheer volume. Yet, optimal mixing is hindered by categorization flaws: human taxonomies suffer from ontological misalignment, and Euclidean clustering fails to address embedding anisotropy. We introduce **GEM** (Geometric Entropy Mixing), a framework reformulating data curation as a variational problem on the hypersphere augmented with a **mixing-balance regularizer**. By decoupling the generative prior and optimizing the objective via a provable **MM (Minorize-Maximize)** algorithm, GEM effectively counteracts the cluster collapse to discover balanced semantic structures invisible to Euclidean heuristics. We employ teacher-student distillation to scale this geometric fidelity to web-scale corpora and introduce the **Geometric Influence Score (GIS)** for interpretable taxonomy generation. Experiments with 1.1B-parameter models demonstrate that GEM establishes a new state-of-the-art when integrated into mixing strategies like DoReMi and RegMix, improving average downstream accuracy by up to **1.2%** and offering a robust coordinate system for predictable data mixing.

1. Introduction

Data curation has emerged as the decisive factor in the performance of Large Language Models (LLMs) (Hoffmann et al., 2022; Gunasekar et al., 2023; Penedo et al., 2023a), shifting the research frontier from sheer parameter scaling to the strategic "mixing" of heterogeneous data sources. As scaling laws (Kaplan et al., 2020) evolve, the core challenge

^{*}Equal contribution ¹Wizard Quant, Beijing, China ²The Hong Kong University of Science and Technology, Hong Kong SAR, China ³Peking University, Beijing, China ⁴University of Science and Technology of China, Hefei, China. Correspondence to: Yue Min <minyue@wizardquant.com>, Yujun Li <liyujun@wizardquant.com>.

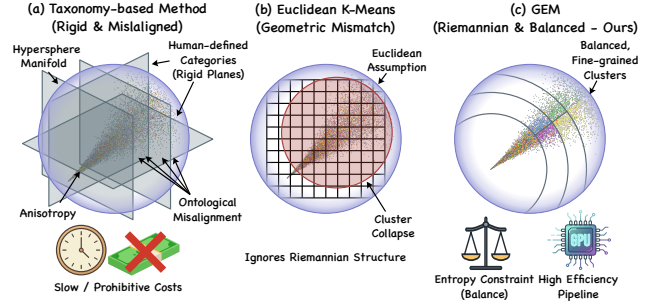


Figure 1. Schematic illustration of geometric mismatch in semantic clustering. While (a) taxonomy-based approaches are hindered by rigid misalignment and high costs, and (b) Euclidean clustering fails to handle embedding anisotropy leading to *cluster collapse*, (c) our proposed GEM framework utilizes MM-based inference to generate balanced, semantically distinct partitions on the hypersphere with superior efficiency.

lies in partitioning massive-scale, unstructured corpora into semantically distinct and balanced clusters, which is a prerequisite for any principled data mixing strategy (Ye et al., 2024). However, contemporary approaches to data classification generally fall into two categories, both of which face fundamental theoretical and practical bottlenecks.

The first category, taxonomy-based methods, relies on human-defined categorical hierarchies (Brown et al., 2020; Touvron et al., 2023b). These approaches typically utilize high-capacity LLMs or ensembles to assign labels to documents. However, as illustrated in Figure 1(a), this paradigm suffers from a critical ontological misalignment: human-centric categories often do not reflect the latent semantic granularity required for self-supervised learning. Empirical evidence suggests that even state-of-the-art models exhibit low inter-annotator consistency when classifying nuanced web data, indicating that human taxonomies fail to capture the true underlying distribution of model-relevant knowledge (Maini et al., 2024; Abbas et al., 2023). Furthermore, the cost of labeling renders this approach unsustainable, especially given the dynamic nature of model development where data is continuously updated, making the constant re-annotation of the corpus operationally prohibitive.

Alternatively, unsupervised approaches like *K*-Means (MacQueen, 1967) provide a scalable option but are predicated on Euclidean geometry. This creates a fundamental mismatch

with modern neural embeddings (e.g., BGE (Xiao et al., 2024), RoBERTa (Liu et al., 2019)), which inherently reside on a high-dimensional hyperspherical manifold optimized for cosine similarity. This geometric discrepancy is exacerbated by *anisotropy*, the so-called “cone effect” (Li et al., 2020), where representations concentrate in narrow, non-uniform sub-regions. Consequently, applying Euclidean clustering to this Riemannian space precipitates “cluster collapse,” as illustrated in Figure 1(b), where dominant clusters swallow the semantic long-tail, severely limiting the diversity requisite for model generalization (Ethayarajh, 2019; Gao et al., 2021).

To bridge this gap, we introduce **GEM (Geometric Entropy Mixing)**, which aligns semantic partitioning with the intrinsic Riemannian geometry of neural representations. As conceptualized in Figure 1(c), GEM departs from Euclidean heuristics by formulating the clustering task as an entropy-regularized variational objective augmented with a mixing-balance regularizer on the unit hypersphere. By explicitly decoupling the generative prior and integrating balance regularizer on empirical mass into the von Mises-Fisher Mixture Model (vMFMM), our method effectively mitigates embedding anisotropy and prevents cluster collapse. This allows GEM to discover fine-grained semantic structures and long-tail distributions that remain latent to traditional distance-based methods, providing a more expressive semantic basis for data mixing. From a systems perspective, GEM is architected for web-scale deployment through a Teacher-Student distillation pipeline that achieves linear time complexity with respect to corpus size. Furthermore, to bridge the gap between geometric clustering and human-centric data curation, we introduce a Geometric Influence Score (GIS)-based sampling method to generate an interpretable, fine-grained taxonomy with descriptions for each semantic category. Extensive experiments demonstrate that the data mixtures derived via GEM consistently yield superior scaling laws, manifesting in lower validation perplexity and enhanced performance across diverse downstream benchmarks compared to competitive baselines.

Our primary contributions are summarized as follows:

- **Geometric formulation with balance regularization.** We propose a hyperspherical variational framework with a novel mixing-balance regularizer to effectively prevent cluster collapse under embedding anisotropy.
- **Provable MM-based inference algorithm.** We derive a provable MM (Minorize-Maximize) algorithm that guarantees monotonic ascent, ensuring stable convergence for the regularized objective.
- **Scalable deployment with interpretability.** We enable linear-time inference via teacher-student distillation and introduce the Geometric Influence Score (GIS) for interpretable taxonomy generation.

- **Consistent gains in data mixing.** Experiments with 1.1B models demonstrate consistent performance gains over strong baselines across diverse benchmarks.

2. Related Work

Data Selection and Mixing for LLMs. Data mixing strategies are pivotal for optimizing LLM training stability and generalization (Brown et al., 2020; Touvron et al., 2023a; Team, 2023). Recent research has introduced adaptive reweighting frameworks. For instance, **DoReMi** (Xie et al., 2023), **DoGE** (Fan et al., 2023), Aioli (Chen et al., 2024) and **RegMix** (Liu et al., 2024) utilize training signals such as gradient alignment, excess loss or performance regression to dynamically adjust domain weights. Extending this granularity, **SampleMix** (Xi et al., 2025) performs evaluation of each individual sample, while **TikMix** (Wang et al., 2025) dynamically recalibrates mixing weights based on data influence. Furthermore, **QuadMix** (Liu et al., 2025) introduces a unified objective to assess both data quality and diversity. Nevertheless, these methods typically treat the underlying categorization as an exogenous constant. Their effectiveness is fundamentally upper-bounded by the quality of the initial partition. If the taxonomy is semantically misaligned or noisy, even these sophisticated mixing algorithms will struggle to isolate high-utility data features. To address this limitation, we argue that refined structural granularity is a prerequisite for effective mixing. We propose a geometry-aware classification scheme that induces semantically coherent partitions from the latent space, enabling robust mixing on high-entropy web data.

Pretraining Data Categorization. Several recent works have explicitly addressed the problem of categorizing large-scale pre-training data, which can be broadly divided into taxonomy-based and unsupervised methods. **Taxonomy-based approaches** rely on predefined label systems and assign categories using supervised classifiers or LLMs. Systems such as WebOrganizer and TnT-LLM employ LLM-based pipelines to annotate web documents into manually designed taxonomies (Wan et al., 2024; Wettig et al., 2025). While these methods yield human-interpretable labels, they suffer from two limitations: (i) the imposed taxonomies reflect human-defined ontologies rather than the latent semantic structure learned by the model, leading to potential ontological misalignment; and (ii) large-scale inference with LLMs incurs substantial computational cost, limiting scalability. **Unsupervised categorization** methods avoid manual labels and instead cluster representations produced by pretrained encoders. Typical techniques include K-Means or density-based clustering algorithms such as HDBSCAN (MacQueen, 1967; McInnes et al., 2017), as adopted in systems like NVIDIA Climb (Diao et al., 2025). Although scalable and label-free, these approaches generally

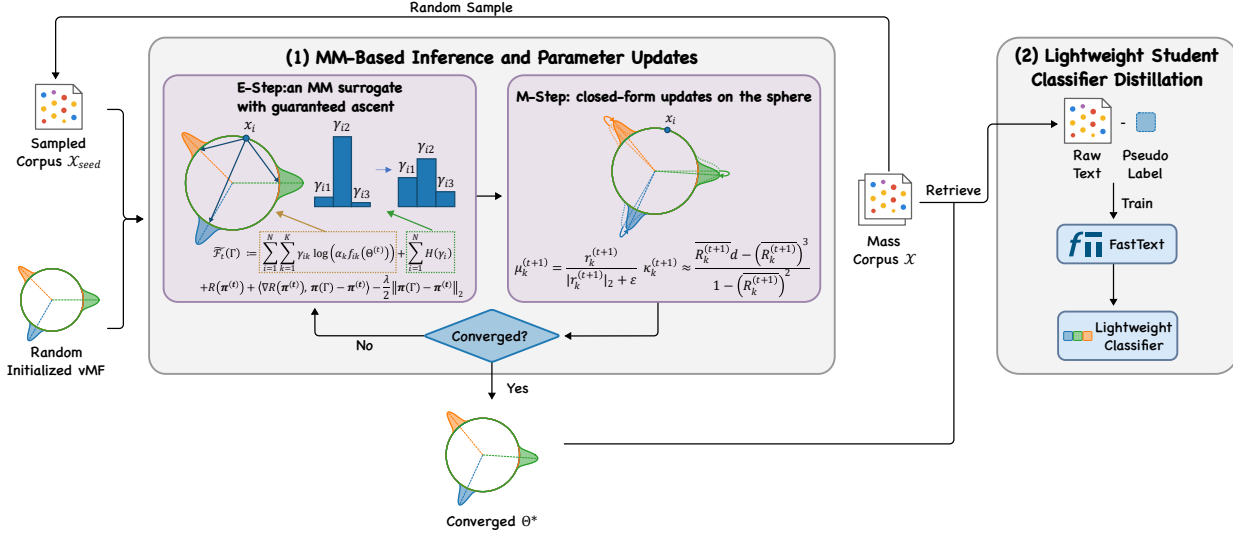


Figure 2. Schematic overview of the GEM framework. The pipeline consists of two phases: **(1) Geometric Optimization (Teacher):** We perform entropy-regularized clustering on the hypersphere using a Mixture of von Mises-Fisher (vMF) distributions. An Minorize–Maximize (MM) algorithm iteratively updates the Riemannian parameters (μ, κ) on a seed corpus \mathcal{X}_{seed} to discover semantic structures. **(2) Scalable Distillation (Student):** The converged geometric partitions are used to pseudo-label the mass corpus \mathcal{X} , guided by GIS score. These labels are then distilled into a lightweight FastText classifier, enabling efficient inference at scale.

operate in Euclidean space and rely on distance-based objectives. In high-dimensional embedding spaces, however, distances tend to concentrate, making Euclidean proximity a weak proxy for semantic similarity.

3. Methodology

We introduce **GEM (Geometric Entropy Mixing)**, a spherical mixture modeling framework for unsupervised semantic partitioning of web-scale text embeddings. GEM is built on directional statistics on the unit hypersphere S^{d-1} and optimizes an entropy-regularized variational objective augmented with an explicit mixing-balance regularizer to mitigate cluster collapse induced by embedding anisotropy. Figure 2 gives an overview. Below, we describe (i) the geometric problem setup, (ii) an entropy-aware vMF mixture formulation with a balance regularizer, (iii) a scalable *MM-based* (minorize–maximize) inference scheme with provable monotonic ascent, (iv) an interpretable taxonomy generation pipeline leveraging Geometric Influence Scores (GIS), and (v) a teacher-student distillation framework for efficient deployment on trillion-token corpora.

3.1. Problem Reformulation

We consider unsupervised semantic partitioning for a massive corpus of normalized text embeddings $\mathcal{X} = \{x_i\}_{i=1}^N \subset \mathbb{R}^d$, where each x_i is ℓ_2 -normalized and thus lies on the unit hypersphere: $x_i \in S^{d-1} := \{x \in \mathbb{R}^d : \|x\|_2 = 1\}$. Our goal is to learn a partition $\mathcal{C} = \{C_1, \dots, C_K\}$ such that clusters are distinguishable by *semantic directionality*,

yielding a robust semantic basis for downstream data mixing in LLM pre-training. This formulation assumes that the directional geometry of the text embedder provides a useful proxy for the downstream LLM’s data geometry. We do not require an exact equivalence between the two spaces; rather, the embedder supplies a stable semantic coordinate system whose utility is empirically validated by data-mixing predictability and downstream pre-training results.

Motivation: concentration on high-dimensional spheres.

A classical concentration phenomenon suggests that Euclidean proximity becomes less informative in high dimensions; on S^{d-1} , angles between random directions concentrate near $\pi/2$.

Lemma 3.1 (Concentration on hyperspheres (Ledoux, 2001)). *Let $x \sim \text{Unif}(S^{d-1})$. For any fixed $p \in S^{d-1}$ and any $\epsilon > 0$,*

$$\mathbb{P}(|\langle x, p \rangle| \leq \epsilon) \geq 1 - 2 \exp\left(-\frac{d\epsilon^2}{2}\right). \quad (1)$$

Remark. Lemma 3.1 provides an intuition that, for $d \gg 1$, random directions are nearly orthogonal. While real neural embeddings are not uniform on S^{d-1} , they often exhibit strong anisotropy and “hubness”, making purely Euclidean clustering unstable. This motivates modeling directional coherence using spherical distributions whose sufficient statistic is cosine similarity.

Variational learning objective. We seek directional parameters Θ and soft assignments $\Gamma = \{\gamma_{ik}\}$ that fit a spherical mixture model while explicitly encouraging *balanced* clus-

ter masses to improve the diversity of induced data mixtures. Let the empirical (soft) cluster mass be

$$\pi_k(\Gamma) := \frac{1}{N} \sum_{i=1}^N \gamma_{ik}, \quad \boldsymbol{\pi}(\Gamma) \in \Delta^{K-1},$$

where $\mathbf{u} := \frac{1}{K} \mathbf{1}$. (2)

We optimize an entropy-regularized variational lower bound (ELBO) augmented with a mixing-balance regularizer:

$$\max_{\Theta, \Gamma} \underbrace{\sum_{i=1}^N \sum_{k=1}^K \gamma_{ik} \log(\alpha_k f_{ik}(\Theta)) + \sum_{i=1}^N H(\gamma_i)}_{\text{Geometric Fidelity (ELBO)}} - \underbrace{\frac{\lambda}{2} \|\boldsymbol{\pi}(\Gamma) - \mathbf{u}\|_2^2}_{\text{Mixing-balance}}, \quad \lambda > 0. \quad (3)$$

where $H(\gamma_i) := -\sum_{k=1}^K \gamma_{ik} \log \gamma_{ik}$ and $f_{ik}(\Theta) := f_{\text{vMF}}(x_i | \mu_k, \kappa_k)$ (defined in Sec. 3.2). Eq. (3) is a tight lower bound of the marginal log-likelihood $\sum_{i=1}^N \log \sum_{k=1}^K \alpha_k f_{ik}(\Theta)$, and becomes exact when γ_i equals the posterior responsibilities. The balance term penalizes deviation from uniform usage of clusters, mitigating degenerate solutions and stabilizing partitions under anisotropic embedding distributions.

3.2. Entropy-Aware Directional Mixture Modeling

von Mises–Fisher (vMF) components. We instantiate the directional likelihood via a mixture of von Mises–Fisher (mvMF) distributions (Banerjee et al., 2005), the canonical directional family on \mathcal{S}^{d-1} . A component k has mean direction $\mu_k \in \mathcal{S}^{d-1}$ and concentration $\kappa_k \geq 0$:

$$f_{\text{vMF}}(x | \mu_k, \kappa_k) = C_d(\kappa_k) \exp(\kappa_k \mu_k^\top x),$$

$$C_d(\kappa_k) = \frac{\kappa_k^{d/2-1}}{(2\pi)^{d/2} I_{d/2-1}(\kappa_k)}, \quad (4)$$

where $I_\nu(\cdot)$ is the modified Bessel function of the first kind. The sufficient statistic $\mu_k^\top x$ is exactly cosine similarity, aligning the generative likelihood with modern embedding metrics.

Decoupling the generative prior from the empirical mass.

To avoid the “rich-get-richer” feedback in standard EM due to learned mixture weights, we fix the generative prior $\alpha_k \equiv 1/K$ for all k . The resulting marginal likelihood is

$$P(x_i | \Theta) = \sum_{k=1}^K \alpha_k f_{\text{vMF}}(x_i | \mu_k, \kappa_k), \quad \alpha_k = \frac{1}{K}. \quad (5)$$

Importantly, the balance regularizer in Eq. (3) acts on the empirical assignment mass $\boldsymbol{\pi}(\Gamma)$, not on the generative prior $\boldsymbol{\alpha}$.

Proposition 3.2 (Concavity, smoothness, and gradient form of the mixing-balance regularizer). *Let $\mathbf{u} := \frac{1}{K} \mathbf{1}$ and define*

$$R(\boldsymbol{\pi}) := -\frac{\lambda}{2} \|\boldsymbol{\pi} - \mathbf{u}\|_2^2, \quad \lambda > 0, \quad (6)$$

for $\boldsymbol{\pi} \in \Delta^{K-1}$. Then R is (i) concave on \mathbb{R}^K (hence also on Δ^{K-1}), (ii) differentiable with gradient

$$\nabla_{\boldsymbol{\pi}_k} R(\boldsymbol{\pi}) = -\lambda(\pi_k - u_k), \quad u_k = \frac{1}{K}, \quad (7)$$

and (iii) λ -smooth with respect to the Euclidean norm, i.e., its gradient is λ -Lipschitz:

$$\|\nabla R(\boldsymbol{\pi}) - \nabla R(\boldsymbol{\pi}')\|_2 \leq \lambda \|\boldsymbol{\pi} - \boldsymbol{\pi}'\|_2, \quad \forall \boldsymbol{\pi}, \boldsymbol{\pi}' \in \mathbb{R}^K. \quad (8)$$

Proof. Expanding Eq. (6) gives $R(\boldsymbol{\pi}) = -\frac{\lambda}{2} \sum_{k=1}^K (\pi_k - u_k)^2$. Differentiating w.r.t. π_k yields Eq. (7). Moreover, R is a negative quadratic function with constant Hessian $\nabla^2 R(\boldsymbol{\pi}) = -\lambda I_K \preceq 0$, which implies concavity on \mathbb{R}^K . Finally, $\nabla R(\boldsymbol{\pi}) = -\lambda(\boldsymbol{\pi} - \mathbf{u})$ is an affine map, hence $\|\nabla R(\boldsymbol{\pi}) - \nabla R(\boldsymbol{\pi}')\|_2 = \lambda \|\boldsymbol{\pi} - \boldsymbol{\pi}'\|_2$, establishing λ -smoothness. \square

3.3. MM-Based Inference and Parameter Updates

Directly maximizing Eq. (3) is nontrivial because $R(\boldsymbol{\pi}(\Gamma))$ couples all samples through the global mass $\boldsymbol{\pi}(\Gamma)$. We therefore derive a scalable minorize–maximize (MM) update that yields a provable monotonic ascent of the objective.

E-step: an MM surrogate with guaranteed ascent. Fix $\Theta = \Theta^{(t)}$ and denote $\boldsymbol{\pi}^{(t)} := \boldsymbol{\pi}(\Gamma^{(t)})$. Since R is concave and λ -smooth, it admits the following global quadratic minorizer: for any $\boldsymbol{\pi}, \boldsymbol{\pi}' \in \Delta^{K-1}$,

$$R(\boldsymbol{\pi}) \geq R(\boldsymbol{\pi}') + \langle \nabla R(\boldsymbol{\pi}'), \boldsymbol{\pi} - \boldsymbol{\pi}' \rangle - \frac{\lambda}{2} \|\boldsymbol{\pi} - \boldsymbol{\pi}'\|_2^2. \quad (9)$$

Applying Eq. (9) with $\boldsymbol{\pi}' = \boldsymbol{\pi}^{(t)}$ and $\boldsymbol{\pi} = \boldsymbol{\pi}(\Gamma)$ yields a tight lower bound of the regularizer at $\Gamma^{(t)}$. Consequently, we define the MM surrogate (a global lower bound that matches the objective at $\Gamma^{(t)}$):

$$\begin{aligned} \tilde{\mathcal{F}}_t(\Gamma) &:= \sum_{i=1}^N \sum_{k=1}^K \gamma_{ik} \log(\alpha_k f_{ik}(\Theta^{(t)})) + \sum_{i=1}^N H(\gamma_i) \\ &+ R(\boldsymbol{\pi}^{(t)}) + \langle \nabla R(\boldsymbol{\pi}^{(t)}), \boldsymbol{\pi}(\Gamma) - \boldsymbol{\pi}^{(t)} \rangle - \frac{\lambda}{2} \|\boldsymbol{\pi}(\Gamma) - \boldsymbol{\pi}^{(t)}\|_2^2. \end{aligned} \quad (10)$$

We then update assignments by maximizing this surrogate:

$$\Gamma^{(t+1)} \in \arg \max_{\Gamma: \gamma_i \in \Delta^{K-1}} \tilde{\mathcal{F}}_t(\Gamma). \quad (11)$$

Monotonicity guarantee. By construction, $\tilde{\mathcal{F}}_t(\Gamma) \leq \mathcal{F}(\Theta^{(t)}, \Gamma)$ for all Γ , and $\tilde{\mathcal{F}}_t(\Gamma^{(t)}) = \mathcal{F}(\Theta^{(t)}, \Gamma^{(t)})$. Therefore, maximizing the surrogate yields a monotonic ascent:

$$\mathcal{F}(\Theta^{(t)}, \Gamma^{(t+1)}) \geq \mathcal{F}(\Theta^{(t)}, \Gamma^{(t)}). \quad (12)$$

A complete monotonic convergence statement for the full GEM iterations is provided in Appendix A.

Practical solver for the MM E-step. The surrogate in Eq. (10) is a concave objective over $\{\gamma_i \in \Delta^{K-1}\}$ (entropy plus a concave quadratic in $\pi(\Gamma)$), and can be efficiently optimized with a few steps of projected (mirror) ascent. In practice, we solve Eq. (11) approximately to a prescribed tolerance; any update that increases $\tilde{\mathcal{F}}_t$ preserves the ascent property in Eq. (12).

M-step: closed-form updates on the sphere. Given $\Gamma^{(t+1)}$, update the empirical mass:

$$\pi_k^{(t+1)} = \frac{1}{N} \sum_{i=1}^N \gamma_{ik}^{(t+1)}. \quad (13)$$

For mean directions, the vMF maximum-likelihood update normalizes the weighted resultant vector:

$$r_k^{(t+1)} = \sum_{i=1}^N \gamma_{ik}^{(t+1)} x_i, \quad \mu_k^{(t+1)} = \frac{r_k^{(t+1)}}{\|r_k^{(t+1)}\|_2 + \varepsilon}, \quad (14)$$

where $\varepsilon > 0$ is a small constant to avoid numerical issues (e.g., near-empty clusters with $\|r_k\| \approx 0$). For concentration parameters, let

$$\bar{R}_k^{(t+1)} := \frac{\|r_k^{(t+1)}\|_2}{\sum_{i=1}^N \gamma_{ik}^{(t+1)}} \in [0, 1), \quad (15)$$

and estimate κ_k using the standard high-dimensional approximation:

$$\kappa_k^{(t+1)} \approx \frac{\bar{R}_k^{(t+1)} d - (\bar{R}_k^{(t+1)})^3}{1 - (\bar{R}_k^{(t+1)})^2}. \quad (16)$$

Summary. GEM combines (i) a spherical vMF mixture with fixed uniform generative prior α and (ii) a mixing-balance regularizer on the empirical mass $\pi(\Gamma)$, optimized via an MM-based E-step with guaranteed monotonic ascent (Eqs. (9)–(12)) and closed-form M-step updates (Eqs. (14)–(16)). This yields semantically coherent yet diverse clusters suitable for robust data mixing in LLM pre-training. The pseudocode of the overall process is provided in Appendix J.

3.4. Interpretable Taxonomy Generation

To transform the unsupervised partition into an interpretable taxonomy for human-understandable data mixing, we employ a Geometric Influence Score (GIS) to select representative samples from each cluster, which are then summarized

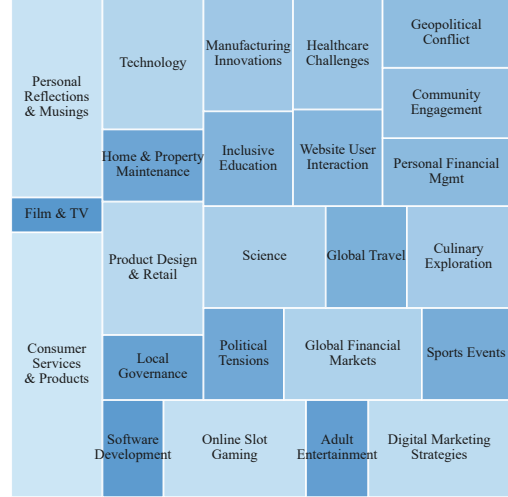


Figure 3. Visualization of the discovered latent semantic taxonomy. The area of each rectangle is proportional to the square root of the number of tokens in that domain within the pre-training corpus.

by LLMs to generate semantic labels. The generated taxonomy is presented in Figure 3. The detailed formulation of GIS and the taxonomy generation process are provided in Appendix B.

3.5. Scalable Deployment of GEM for Data Mixing

Direct application of GEM to trillion-token corpora is computationally prohibitive due to the cost of iterative EM optimization. We bridge this gap using a Teacher-Student distillation framework. In this framework, GEM serves as the “Teacher,” operating on a representative seed corpus to discover latent semantic structures. We then utilize the proposed Geometric Influence Score (GIS) to curate a high-confidence, balanced training set from these clusters. This dataset supervises a “Student” model, a lightweight linear classifier which approximates the GEM-induced partition function. This design aligns with established industry practices for processing web-scale data, where linear classifiers are preferred for their strict latency constraints (Wenzek et al., 2020; Soldaini et al., 2024). By distilling the hyperspherical geometry into a fast inference model, we enable semantic partitioning over the full pre-training corpus with negligible computational overhead. Detailed procedures for the clustering, pseudo-labeling, and distillation phases are provided in Appendix C.

4. Experiments

In this section, we evaluate the effectiveness of our proposed taxonomy in the context of large-scale data mixing. We aim to demonstrate that our classification scheme provides a more granular and semantically coherent partitioning of web data, leading to superior downstream model performance

GEM: Geometric Entropy Mixing for Optimal LLM Data Curation

Table 1. Main results on downstream tasks. We compare our **GEM** sampling strategy against baseline methods (K-Means, Spherical K-Means, TOS) and existing semantic organizers (WebOrganizer) across three different pre-training frameworks. The best results within each group are highlighted in **bold**, and the second best results are highlighted by underline.

Model Variation	Science QA	Commonsense Reasoning	Logic & Linguistics	Average
Under DoReMi				
K-Means	32.18	34.21	53.43	39.94
Spherical K-Means	34.62	<u>38.97</u>	54.72	42.77
TOS	32.49	34.29	53.98	40.25
WebOrganizer Topic	<u>34.68</u>	38.26	<u>55.35</u>	42.76
WebOrganizer Format	34.44	38.73	55.19	<u>42.79</u>
GEM (Ours)	34.79	39.96	57.11	43.95
Under Perf				
K-Means	32.48	35.11	55.52	41.04
Spherical K-Means	34.56	<u>39.95</u>	53.85	42.78
TOS	32.54	34.51	53.29	40.11
WebOrganizer Topic	35.05	39.73	57.90	44.23
WebOrganizer Format	<u>35.06</u>	39.73	<u>57.97</u>	<u>44.25</u>
GEM (Ours)	35.96	40.43	57.98	44.79
Under RegMix				
K-Means	31.63	<u>34.86</u>	55.67	40.72
Spherical K-Means	32.58	<u>34.86</u>	54.47	40.63
TOS	32.18	34.35	52.40	39.64
WebOrganizer Topic	33.90	33.83	52.50	40.08
WebOrganizer Format	34.12	33.94	54.26	<u>40.77</u>
GEM (Ours)	<u>34.07</u>	35.30	<u>54.97</u>	41.45

when combined with various data selection and reweighting algorithms.

4.1. Experimental Settings

Datasets and Models. To systematically investigate the effectiveness of data classification for data mixing on unlabeled web-scale corpora, we construct our pre-training dataset from raw CommonCrawl (CC) (Raffel et al., 2020) data. We apply a rigorous cleaning and filtering pipeline that closely follows the protocols established in Refined-Web (Penedo et al., 2023b), ensuring high-quality and noise-reduced training data. We adopt a LLaMA-style Transformer architecture (Touvron et al., 2023a) with 1.1B parameters. The model configuration is trained with a fixed compute budget of 25 billion tokens to ensure fair and controlled comparisons across different data mixing strategies. Details of the pre-training hyperparameters and experimental infrastructure are provided in Appendix D.

Categorization Baselines. We compare our proposed taxonomy against several established data organization paradigms: (1) **TOS** (Peng et al., 2025), which employs a human-

curated hierarchical semantic structure for domain partitioning; (2) **WebOrganizer (Topic)** and (3) **WebOrganizer (Format)**, which leverage LLM-derived topic labels and structural layout features, respectively (Wettig et al., 2025); (4) **K-means** (MacQueen, 1967), an unsupervised clustering baseline that partitions data based on document-level embeddings; and (5) **Spherical K-Means**, which replaces Euclidean distance with cosine geometry while retaining hard assignments. Details for implementation and training are provided in Appendix E.

GEM Hyperparameters. Unless otherwise noted, we set $K = 24$ and $\lambda = 5000$ in the main experiments. The value of λ is chosen by aligning the balance regularizer with the assignment-logit scale induced by the vMF likelihood, whose learned concentrations are typically around $\kappa \approx 900$. We provide sensitivity analyses for both λ and the seed-corpus size in Appendix I.

Data Mixing Strategies. To evaluate the downstream utility of these taxonomies, we integrate them with the following mixing algorithms: (1) **Perf**, which utilizes a sensitivity-driven approach by upsampling high-impact categories iden-

tified through preliminary performance gains (Peng et al., 2025); (2) **RegMix**, which formulates data mixing as a regression task to predict model performance across different distribution vectors (Liu et al., 2024); and (3) **DoReMi**, which exploits a distributionally robust optimization objective to minimize the maximum excess loss via a proxy model (Xie et al., 2023). We provide the detailed search space and computational budgets for ratio optimization in Appendix F.

Downstream Task Evaluation. We evaluate the zero-shot generalization capabilities of our pre-trained models using the **OLMES** (Gu et al., 2025) framework across nine benchmark datasets. To provide a granular analysis of model performance, we categorize these benchmarks into three core dimensions: (1) **Science QA**: ARC-Challenge (Clark et al., 2018), ARC-Easy (Clark et al., 2018), SciQ (Welbl et al., 2017), and OpenBookQA (Mihaylov et al., 2018). (2) **Commonsense Reasoning**: HellaSwag (Zellers et al., 2019), PIQA (Bisk et al., 2020), and CommonsenseQA (Talmor et al., 2019). (3) **Logic & Linguistics**: WinoGrande (Sakaguchi et al., 2021) and COPA (Roemmele et al., 2011). By adhering to the standardized evaluation matrix in OLMES (Gu et al., 2025), we ensure consistency in prompt templates and scoring metrics.

4.2. Main Results

We evaluate the effectiveness of our proposed method by integrating the GEM-based taxonomy into three distinct data mixing frameworks: DoReMi, Perf, and RegMix. Table 1 presents the comparative performance across three aggregated capabilities and the overall average.

Downstream Performance Analysis. The empirical results presented in Table 1 substantiate the effectiveness of our proposed GEM strategy, which consistently achieves superior performance across diverse data mixing frameworks. Specifically, under the **DoReMi** framework, GEM exhibits the most pronounced improvements, surpassing the strongest baseline, WebOrganizer, by substantial margins of 1.23% and 1.76% points on Commonsense Reasoning and Logic & Linguistics, respectively. This trend persists within the **Perf** framework, where GEM establishes best results in Science QA and Commonsense Reasoning, while maintaining a competitive edge in Logic & Linguistics by attaining a score of 57.98% compared to the 57.97% achieved by the runner-up. In the **RegMix** setting, although the K-Means baseline holds a marginal advantage in Logic & Linguistics with a performance of 55.67%, GEM remains dominant in Science QA and Commonsense Reasoning, significantly outperforming other semantic-aware organizers. Collectively, these results underscore the robustness of GEM in selecting high-value training samples that enhance model reasoning capabilities independent of the underlying mixing strategy.

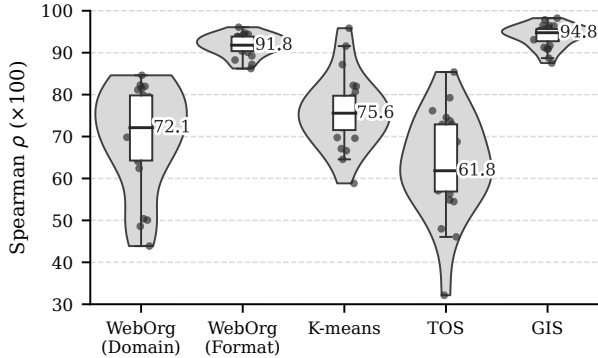


Figure 4. Downstream loss predictability across taxonomies. Violin plots show per-subcategory Spearman correlation (ρ) between RegMix and ground-truth validation loss, averaged over 10 splits. Dots: subcategories; Boxes: Median/IQR; Whiskers: $1.5 \times$ IQR.

Evaluating Taxonomy Quality via Data Mixing Predictability. A robust taxonomy for data mixing must yield well-conditioned mixing coordinates, where small adjustments to mixture weights induce consistent and predictable shifts in validation loss. We quantify this property using **RegMix** (Liu et al., 2024) as a *predictability probe*. Specifically, we measure the Spearman rank correlation (ρ) between the ground-truth validation loss and the loss predicted by RegMix on held-out mixture vectors (implementation details in Appendix G). To reduce variance due to a particular split of mixture vectors, we repeat the procedure over 10 independent train/test splits and report, for each sub-taxonomy unit, the average ρ across splits. As illustrated in Figure 4, the choice of taxonomy significantly impacts predictability. Baselines such as K-Means and WebOrganizer exhibit lower and more dispersed ρ values, indicating unstable mixing dynamics dominated by redundant or entangled factors. In contrast, **GEM** demonstrates superior predictability, achieving consistently higher ρ with a notably tighter distribution. This reduction in variance suggests that GEM induces a taxonomy with minimized factor entanglement and a smoother optimization landscape, thereby enabling more sample-efficient mixture search and reliable control over data composition during pre-training.

Impact of Cluster Granularity. In our primary experiments, we set the number of clusters to $K = 24$ to ensure a controlled comparison across all baselines. To further investigate the optimal granularity for the GIS module, we conduct a sensitivity analysis by varying K from 12 to 48. As illustrated in Figure 5, the model performance manifests a clear dependence on cluster density. Specifically, we observe a consistent performance trajectory that peaks at $K = 36$, achieving an *Average* score of 41.21%. This trend suggests that increasing cluster granularity facilitates the capture of more refined latent semantic patterns. However, performance begins to plateau or slightly degrade as

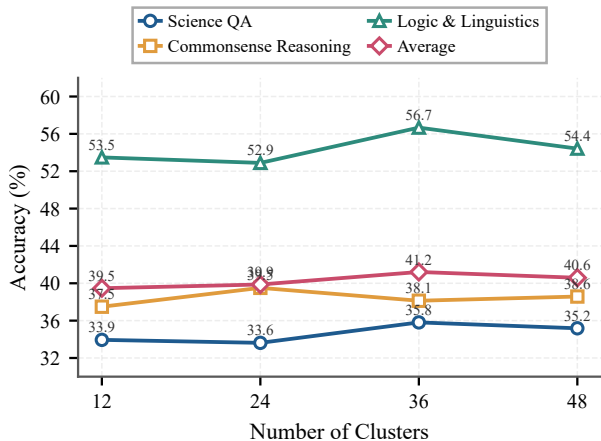


Figure 5. Sensitivity to the number of clusters K . Accuracy (%) on Science QA, Commonsense Reasoning, Logic & Linguistics, and Average as K varies from 12 to 48 (GEM + Perf.)

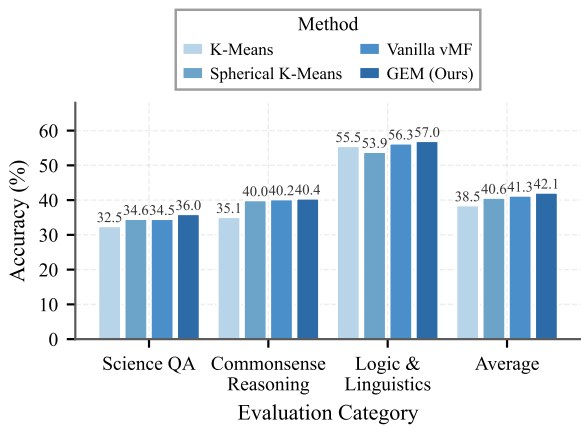


Figure 6. Ablation study on clustering mechanisms. The results highlight the improvements gained by shifting from Euclidean to Riemannian geometry and by incorporating regularizer.

K reaches 48. This marginal decline is likely attributable to the over-fragmentation of the embedding space, where excessive partitioning may introduce stochastic noise or impede the model’s ability to derive robust, generalized representations.

4.3. Ablation Study

To rigorously assess the contribution of each component within our framework, we perform an ablation study comparing GEM against three baseline variants: K-Means, Spherical K-Means (Hyperspherical geometry with hard assignments), and Vanilla vMF (Riemannian geometry without regularizer). As visualized in Figure 6, the results exhibit a monotonic performance improvement that aligns with the theoretical fidelity of the clustering objective. The standard K-Means baseline yields the lowest average accuracy of 38.5%, corroborating the limitations of Euclidean metrics

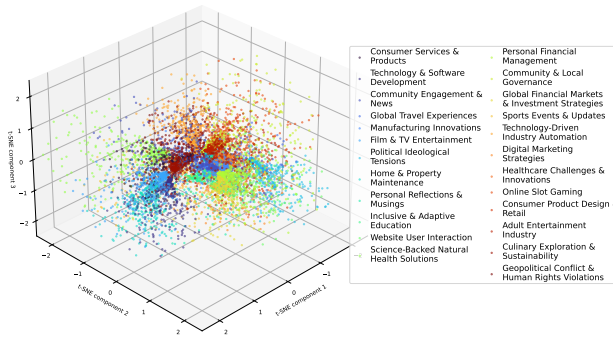


Figure 7. t-SNE visualization of GEM-induced clusters (3D). Colors denote the 24 taxonomy topics generated by GIS-based sampling and LLM summarization.

in high-dimensional embedding spaces. Transitioning to Spherical K-Means increases the average accuracy to 40.6%. Vanilla vMF further elevates performance to 41.3% by leveraging probabilistic soft assignments to capture semantic nuances. Crucially, the proposed GEM framework achieves the highest average accuracy of 42.1%, with notable gains in Science QA at 36.0% and Logic & Linguistics at 57.0%. These findings confirm that the gradient-consistent entropy constraint is essential for mitigating anisotropic cluster collapse, thereby ensuring a semantically balanced taxonomy that facilitates robust downstream generalization.

5. Discussion

A key message of GEM is that “better” categorization for LLM data mixing should be evaluated not only by human interpretability, but by whether the induced coordinates make mixture search controllable and predictable. Our RegMix-based predictability probe (Figure 4) indicates that GEM yields a better-conditioned mixing simplex—small weight perturbations produce more consistent loss orderings—suggesting reduced factor entanglement relative to Euclidean heuristics. Although GEM clusters are unlabeled, GIS-guided representative selection makes interpretability a practical byproduct rather than a fragile post-hoc step: the t-SNE visualization (Figure 7) shows multiple discernible local neighborhoods alongside overlap in dense regions, reflecting genuine semantic proximity among discovered topics rather than mere labeling noise.

Several avenues remain for future exploration. First, the current 1.1B-parameter, 25B-token setting should be interpreted as an early-stage scaling indicator; extending GEM to multi-trillion-token regimes and diverse model architectures remains necessary to further validate its scaling properties. Second, investigating GIS as a standalone data curation primitive can clarify its efficacy in prioritizing high-signal samples beyond mere partitioning. Third, deployment on

continuously updated web corpora should monitor distribution shifts such as AI-generated content contamination; we provide a preliminary robustness analysis in Appendix I.1. Finally, exploring the co-optimization of taxonomy discovery and downstream objectives offers a compelling direction; such bi-level optimization frameworks could enable a self-improving cycle where the semantic basis and model performance mutually adapt to enhance task-specific generalization.

6. Conclusion

We presented **GEM (Geometric Entropy Mixing)**, a geometry-aware framework for unsupervised data categorization that aligns semantic partitioning with hyperspherical embedding structures. By combining a vMF mixture model with an explicit mixing-balance regularizer and an MM-based inference scheme with monotonic ascent, GEM mitigates anisotropy-induced cluster collapse and yields semantically coherent yet balanced partitions. To scale to web-scale corpora, we distill GEM’s decisions into a lightweight classifier and employ GIS-guided sampling for interpretable taxonomies. Extensive experiments with 1.1B-parameter models show that GEM consistently improves downstream performance across multiple mixing frameworks. GEM offers a principled foundation for future work on jointly optimizing taxonomy discovery and data mixture learning.

Impact Statement

This paper presents work whose goal is to advance the field of Machine Learning. There are many potential societal consequences of our work, none which we feel must be specifically highlighted here.

References

- Abbas, A., Tirumala, K., Simig, D., Ganguli, S., and Morcos, A. S. Semdedup: Data-efficient learning at web-scale through semantic deduplication. *arXiv preprint arXiv:2303.09540*, 2023.
- Banerjee, A., Dhillon, I. S., Ghosh, J., Sra, S., and Ridgeway, G. Clustering on the unit hypersphere using von mises-fisher distributions. *Journal of Machine Learning Research*, 6(9), 2005.
- Ben Allal, L., Lozhkov, A., Penedo, G., Wolf, T., and von Werra, L. Cosmopedia, 2024. URL <https://huggingface.co/datasets/HuggingFaceTB/cosmopedia>.
- Bisk, Y., Zellers, R., Gao, J., Choi, Y., et al. Piqa: Reasoning about physical commonsense in natural language. In *Proceedings of the AAAI conference on artificial intelligence*, volume 34, pp. 7432–7439, 2020.
- Brown, T., Mann, B., Ryder, N., Subbiah, M., Kaplan, J. D., Dhariwal, P., Neelakantan, A., Shyam, P., Sastry, G., Askell, A., et al. Language models are few-shot learners. *Advances in neural information processing systems*, 33: 1877–1901, 2020.
- Chen, M. F., Hu, M. Y., Lourie, N., Cho, K., and Ré, C. Aioli: A unified optimization framework for language model data mixing. *arXiv preprint arXiv:2411.05735*, 2024.
- Clark, P., Cowhey, I., Etzioni, O., Khot, T., Sabharwal, A., Schoenick, C., and Tafjord, O. Think you have solved question answering? try arc, the ai2 reasoning challenge. *arXiv preprint arXiv:1803.05457*, 2018.
- Diao, S., Yang, Y., Fu, Y., Dong, X., Su, D., Kliegl, M., Chen, Z., Belcak, P., Suhara, Y., Yin, H., et al. Climb: Clustering-based iterative data mixture bootstrapping for language model pre-training. *arXiv preprint arXiv:2504.13161*, 2025.
- Ethayarajh, K. How contextual are contextualized word representations? comparing the geometry of bert, elmo, and gpt-2 embeddings. *arXiv preprint arXiv:1909.00512*, 2019.
- Fan, S., Pagliardini, M., and Jaggi, M. Doge: Domain reweighting with generalization estimation. *arXiv preprint arXiv:2310.15393*, 2023.
- Gao, T., Yao, X., and Chen, D. Simcse: Simple contrastive learning of sentence embeddings. *arXiv preprint arXiv:2104.08821*, 2021.
- Gu, Y., Tafjord, O., Kuehl, B., Haddad, D., Dodge, J., and Hajishirzi, H. Olmes: A standard for language model evaluations. In *Findings of the Association for Computational Linguistics: NAACL 2025*, pp. 5005–5033, 2025.
- Gunasekar, S., Zhang, Y., Aneja, J., Mendes, C. C. T., Del Giorno, A., Gopi, S., Javaheripi, M., Kauffmann, P., de Rosa, G., Saarikivi, O., et al. Textbooks are all you need. *arXiv preprint arXiv:2306.11644*, 2023.
- Hans, A., Schwarzschild, A., Cherepanova, V., Kazemi, H., Saha, A., Goldblum, M., Geiping, J., and Goldstein, T. Spotting llms with binoculars: Zero-shot detection of machine-generated text. *arXiv preprint arXiv:2401.12070*, 2024.
- Hoffmann, J., Borgeaud, S., Mensch, A., Buchatskaya, E., Cai, T., Rutherford, E., Casas, D. d. L., Hendricks, L. A., Welbl, J., Clark, A., et al. Training compute-optimal large language models. *arXiv preprint arXiv:2203.15556*, 2022.

- Joulin, A., Grave, E., Bojanowski, P., and Mikolov, T. Bag of tricks for efficient text classification. In *Proceedings of the 15th conference of the European chapter of the association for computational linguistics: volume 2, short papers*, pp. 427–431, 2017.
- Kaplan, J., McCandlish, S., Henighan, T., Brown, T. B., Chess, B., Child, R., Gray, S., Radford, A., Wu, J., and Amodei, D. Scaling laws for neural language models. *arXiv preprint arXiv:2001.08361*, 2020.
- Ledoux, M. *The concentration of measure phenomenon*. Number 89. American Mathematical Soc., 2001.
- Li, B., Zhou, H., He, J., Wang, M., Yang, Y., and Li, L. On the sentence embeddings from pre-trained language models. *arXiv preprint arXiv:2011.05864*, 2020.
- Liu, F., Zhou, W., Liu, B., Yu, Z., Zhang, Y., Lin, H., Yu, Y., Zhang, B., Zhou, X., Wang, T., et al. Quadmix: Quality-diversity balanced data selection for efficient llm pretraining. *arXiv preprint arXiv:2504.16511*, 2025.
- Liu, Q., Zheng, X., Muennighoff, N., Zeng, G., Dou, L., Pang, T., Jiang, J., and Lin, M. Regmix: Data mixture as regression for language model pre-training. *arXiv preprint arXiv:2407.01492*, 2024.
- Liu, Y., Ott, M., Goyal, N., Du, J., Joshi, M., Chen, D., Levy, O., Lewis, M., Zettlemoyer, L., and Stoyanov, V. Roberta: A robustly optimized bert pretraining approach. *arXiv preprint arXiv:1907.11692*, 2019.
- MacQueen, J. Multivariate observations. In *Proceedings of the 5th Berkeley Symposium on Mathematical Statistics and Probability*, volume 1, pp. 281–297, 1967.
- Maini, P., Seto, S., Bai, R., Grangier, D., Zhang, Y., and Jaitly, N. Rephrasing the web: A recipe for compute and data-efficient language modeling. In *Proceedings of the 62nd Annual Meeting of the Association for Computational Linguistics (Volume 1: Long Papers)*, pp. 14044–14072, 2024.
- McInnes, L., Healy, J., Astels, S., et al. hdbscan: Hierarchical density based clustering. *J. Open Source Softw.*, 2(11):205, 2017.
- Mihaylov, T., Clark, P., Khot, T., and Sabharwal, A. Can a suit of armor conduct electricity? a new dataset for open book question answering. *arXiv preprint arXiv:1809.02789*, 2018.
- Penedo, G., Malartic, Q., Hesslow, D., Cojocaru, R., Cappelli, A., Alobeidli, H., Pannier, B., Almazrouei, E., and Launay, J. The refinedweb dataset for falcon llm: outperforming curated corpora with web data, and web data only. *arXiv preprint arXiv:2306.01116*, 2023a.
- Penedo, G., Malartic, Q., Hesslow, D., Cojocaru, R., Cappelli, A., Alobeidli, H., Pannier, B., Almazrouei, E., and Launay, J. The refinedweb dataset for falcon llm: outperforming curated corpora with web data, and web data only. *arXiv preprint arXiv:2306.01116*, 2023b.
- Peng, J., Zhuang, X., Qiu, J., Ma, R., Yu, J., Zhu, H., and He, C. Topic over source: The key to effective data mixing for language models pre-training, 2025. URL <https://arxiv.org/abs/2502.16802>.
- Raffel, C., Shazeer, N., Roberts, A., Lee, K., Narang, S., Matena, M., Zhou, Y., Li, W., and Liu, P. J. Exploring the limits of transfer learning with a unified text-to-text transformer. *Journal of machine learning research*, 21(140):1–67, 2020.
- Roemmele, M., Bejan, C. A., and Gordon, A. S. Choice of plausible alternatives: An evaluation of commonsense causal reasoning. In *AAAI spring symposium: logical formalizations of commonsense reasoning*, pp. 90–95, 2011.
- Sakaguchi, K., Bras, R. L., Bhagavatula, C., and Choi, Y. Winogrande: an adversarial winograd schema challenge at scale. *Commun. ACM*, 64(9):99–106, August 2021. ISSN 0001-0782. doi: 10.1145/3474381. URL <https://doi.org/10.1145/3474381>.
- Soldaini, L., Kinney, R., Bhagia, A., Schwenk, D., Atkinson, D., Authur, R., Bogin, B., Chandu, K., Dumas, J., Elazar, Y., et al. Dolma: An open corpus of three trillion tokens for language model pretraining research. In *Proceedings of the 62nd annual meeting of the association for computational linguistics (volume 1: long papers)*, pp. 15725–15788, 2024.
- Talmor, A., Herzig, J., Lourie, N., and Berant, J. Commonsenseqa: A question answering challenge targeting commonsense knowledge. In *Proceedings of the 2019 Conference of the North American Chapter of the Association for Computational Linguistics: Human Language Technologies, Volume 1 (Long and Short Papers)*, pp. 4149–4158, 2019.
- Team, I. Internlm: A multilingual language model with progressively enhanced capabilities, 2023.
- Touvron, H., Llavrit, T., Izacard, G., Martinet, X., Lachaux, M.-A., Lacroix, T., Rozière, B., Goyal, N., Hambro, E., Azhar, F., et al. Llama: Open and efficient foundation language models. *arXiv preprint arXiv:2302.13971*, 2023a.
- Touvron, H., Martin, L., Stone, K., Albert, P., Almahairi, A., Babaei, Y., Bashlykov, N., Batra, S., Bhargava, P., Bhosale, S., et al. Llama 2: Open foundation and fine-tuned chat models. *arXiv preprint arXiv:2307.09288*, 2023b.

- Wan, M., Safavi, T., Jauhar, S. K., Kim, Y., Counts, S., Neville, J., Suri, S., Shah, C., White, R. W., Yang, L., et al. Tnt-llm: Text mining at scale with large language models. In *Proceedings of the 30th ACM SIGKDD conference on knowledge discovery and data mining*, pp. 5836–5847, 2024.
- Wang, Y., Liu, B., Liu, F., Guo, Y., Deng, J., Wu, X., Zhou, W., Zhou, X., and Wang, T. Tikmix: Take data influence into dynamic mixture for language model pre-training. *arXiv preprint arXiv:2508.17677*, 2025.
- Welbl, J., Liu, N. F., and Gardner, M. Crowdsourcing multiple choice science questions. *arXiv preprint arXiv:1707.06209*, 2017.
- Wenzek, G., Lachaux, M.-A., Conneau, A., Chaudhary, V., Guzmán, F., Joulin, A., and Grave, E. Ccnet: Extracting high quality monolingual datasets from web crawl data. In *Proceedings of the twelfth language resources and evaluation conference*, pp. 4003–4012, 2020.
- Wettig, A., Lo, K., Min, S., Hajishirzi, H., Chen, D., and Soldaini, L. Organize the web: Constructing domains enhances pre-training data curation. *arXiv preprint arXiv:2502.10341*, 2025.
- Xi, X., Kong, D., Yang, J., Yang, J., Chen, Z., Wang, W., Wang, J., Cai, X., Zhang, S., and Ye, W. Samplemix: A sample-wise pre-training data mixing strategy by coordinating data quality and diversity. *arXiv preprint arXiv:2503.01506*, 2025.
- Xiao, S., Liu, Z., Zhang, P., Muennighoff, N., Lian, D., and Nie, J.-Y. C-pack: Packed resources for general chinese embeddings. In *Proceedings of the 47th international ACM SIGIR conference on research and development in information retrieval*, pp. 641–649, 2024.
- Xie, S. M., Pham, H., Dong, X., Du, N., Liu, H., Lu, Y., Liang, P. S., Le, Q. V., Ma, T., and Yu, A. W. Doremi: Optimizing data mixtures speeds up language model pre-training. *Advances in Neural Information Processing Systems*, 36:69798–69818, 2023.
- Ye, J., Liu, P., Sun, T., Zhan, J., Zhou, Y., and Qiu, X. Data mixing laws: Optimizing data mixtures by predicting language modeling performance. *arXiv preprint arXiv:2403.16952*, 2024.
- Zellers, R., Holtzman, A., Bisk, Y., Farhadi, A., and Choi, Y. Hellaswag: Can a machine really finish your sentence? *arXiv preprint arXiv:1905.07830*, 2019.

A. Monotonic Convergence of GEM

Monotonic ascent guarantee.

Theorem A.1 (Monotonic convergence of GEM). *Let $\mathcal{F}(\Theta, \Gamma)$ denote the GEM objective in Eq. (3). Fix an iteration t and construct the MM surrogate $\tilde{\mathcal{F}}_t(\Gamma)$ as in Eq. (10) using $\boldsymbol{\pi}^{(t)} := \boldsymbol{\pi}(\Gamma^{(t)})$. Assume the E-step returns $\Gamma^{(t+1)}$ such that*

$$\tilde{\mathcal{F}}_t(\Gamma^{(t+1)}) \geq \tilde{\mathcal{F}}_t(\Gamma^{(t)}), \quad (17)$$

and the M-step returns $\Theta^{(t+1)}$ such that

$$\mathcal{F}(\Theta^{(t+1)}, \Gamma^{(t+1)}) \geq \mathcal{F}(\Theta^{(t)}, \Gamma^{(t+1)}). \quad (18)$$

Then GEM produces a monotone non-decreasing sequence of objective values:

$$\mathcal{F}(\Theta^{(t+1)}, \Gamma^{(t+1)}) \geq \mathcal{F}(\Theta^{(t)}, \Gamma^{(t)}), \quad \forall t \geq 0. \quad (19)$$

Consequently, if \mathcal{F} is upper bounded on the feasible set, the sequence $\{\mathcal{F}(\Theta^{(t)}, \Gamma^{(t)})\}_{t \geq 0}$ converges to a finite limit.

Proof. We first show that $\tilde{\mathcal{F}}_t$ is a valid minorizer of $\Gamma \mapsto \mathcal{F}(\Theta^{(t)}, \Gamma)$. Let $R(\boldsymbol{\pi}) := -\frac{\lambda}{2} \|\boldsymbol{\pi} - \mathbf{u}\|_2^2$. By Proposition 3.2, R is concave and λ -smooth, hence it satisfies the global quadratic minorization inequality in Eq. (9), i.e., for all $\boldsymbol{\pi} \in \Delta^{K-1}$,

$$R(\boldsymbol{\pi}) \geq R(\boldsymbol{\pi}^{(t)}) + \langle \nabla R(\boldsymbol{\pi}^{(t)}), \boldsymbol{\pi} - \boldsymbol{\pi}^{(t)} \rangle - \frac{\lambda}{2} \|\boldsymbol{\pi} - \boldsymbol{\pi}^{(t)}\|_2^2.$$

Substituting $\boldsymbol{\pi} = \boldsymbol{\pi}(\Gamma)$ yields, for all feasible Γ ,

$$\tilde{\mathcal{F}}_t(\Gamma) \leq \mathcal{F}(\Theta^{(t)}, \Gamma), \quad \tilde{\mathcal{F}}_t(\Gamma^{(t)}) = \mathcal{F}(\Theta^{(t)}, \Gamma^{(t)}), \quad (20)$$

where the equality follows because $\boldsymbol{\pi}(\Gamma^{(t)}) = \boldsymbol{\pi}^{(t)}$ makes Eq. (9) tight.

Using Eq. (20) and the E-step condition (17), we obtain

$$\mathcal{F}(\Theta^{(t)}, \Gamma^{(t+1)}) \geq \tilde{\mathcal{F}}_t(\Gamma^{(t+1)}) \geq \tilde{\mathcal{F}}_t(\Gamma^{(t)}) = \mathcal{F}(\Theta^{(t)}, \Gamma^{(t)}).$$

Finally, applying the M-step condition (18) gives

$$\mathcal{F}(\Theta^{(t+1)}, \Gamma^{(t+1)}) \geq \mathcal{F}(\Theta^{(t)}, \Gamma^{(t+1)}) \geq \mathcal{F}(\Theta^{(t)}, \Gamma^{(t)}),$$

which proves Eq. (19). If \mathcal{F} is upper bounded on the feasible set, any monotone non-decreasing sequence $\{\mathcal{F}(\Theta^{(t)}, \Gamma^{(t)})\}_{t \geq 0}$ converges to a finite limit. \square

B. Interpretability Analysis: GIS and Taxonomy Details

B.1. Interpretability Sampling via GIS

Unsupervised clustering yields a partition function $x_i \mapsto \arg \max_k \gamma_{ik}$, but the resulting cluster indices are not directly human-interpretable. To enable domain-level control in downstream data mixing (e.g., “increase Math by 10%”), we convert each cluster into a semantic label by prompting an LLM with a small set of *representative* samples from that cluster. The key challenge is that naive random sampling often selects either boundary points (ambiguous assignments) or geometrically central but semantically isolated points under anisotropic embedding distributions. We therefore propose a principled selection criterion, the **Geometric Influence Score (GIS)**, that is consistent with the GEM objective in Sec. 3.

Definition. Let Γ and $\Theta = \{(\mu_k, \kappa_k)\}_{k=1}^K$ be the learned GEM assignments and vMF parameters (Sec. 3.2–3.3). For a sample x_i and cluster k , define the *cluster-conditional GIS* as

$$\text{GIS}_k(x_i) := \underbrace{\log(\gamma_{ik} + \varepsilon)}_{\text{certainty}} + \underbrace{\log f_{\text{vMF}}(x_i \mid \mu_k, \kappa_k)}_{\text{directional coherence}} + \underbrace{\beta \log(\rho_k(x_i) + \varepsilon)}_{\text{local support}}, \quad (21)$$

where $\varepsilon > 0$ is a small constant for numerical stability and $\beta \geq 0$ controls the strength of the density term.

Using the vMF likelihood defined in Sec. 3.2,

$$\log f_{\text{vMF}}(x_i | \mu_k, \kappa_k) = \log C_d(\kappa_k) + \kappa_k \mu_k^\top x_i. \quad (22)$$

Since $\log C_d(\kappa_k)$ is independent of i for fixed k , ranking samples *within the same cluster* is equivalent to using $\kappa_k \mu_k^\top x_i$; we keep the full $\log f_{\text{vMF}}$ in Eq. (21) to make the probabilistic meaning explicit and to remain fully consistent with the generative model.

To penalize semantically isolated points, we estimate a cluster-aware local density by restricting neighbors to the same cluster:

$$\rho_k(x_i) := \frac{1}{M} \sum_{x_j \in \mathcal{N}_M^{(k)}(x_i)} x_i^\top x_j, \quad \mathcal{N}_M^{(k)}(x_i) \subseteq \{x_j : \arg \max_\ell \gamma_{j\ell} = k\}, \quad (23)$$

where $\mathcal{N}_M^{(k)}(x_i)$ denotes the M nearest neighbors of x_i *within cluster k* under cosine similarity (equivalently Euclidean distance on \mathcal{S}^{d-1}). This cluster-restricted density avoids cross-cluster contamination and directly measures whether x_i lies in a densely populated region of the learned semantic direction.

For each cluster k , we select representatives by ranking points assigned to k using $\text{GIS}_k(x_i)$ and taking the top- S samples:

$$\mathcal{R}_k := \text{TopS} \left(\{\text{GIS}_k(x_i)\}_{i: \arg \max_\ell \gamma_{i\ell} = k} \right). \quad (24)$$

The set \mathcal{R}_k is then used as few-shot context to prompt an LLM for a concise semantic label, yielding an interpretable taxonomy consistent with the GEM-induced partition.

B.2. GIS Taxonomy Details

B.2.1. TAXONOMY DESCRIPTION

Table 2 provides a comprehensive overview of the semantic taxonomies identified by our GEM framework. Each taxonomy represents a distinct semantic cluster discovered through our entropy-regularized vMF mixture modeling approach, enabling fine-grained categorization of the pre-training corpus for optimal data mixing strategies.

Table 2. Detailed overview of our topic definitions. This table lists the specific topics and their corresponding descriptions to decrease uncertainty and define domain boundaries.

Taxonomy	Description
Consumer Services and Products	This topic encompasses a range of services and products aimed at improving consumer experiences, emphasizing sustainability, marketing, and quality in various industries.
Technology and Software Development	This topic encompasses the development, functionality, and improvement of software and technology solutions, focusing on web development, software tools, and user experience enhancements.
Community Engagement and News	The topic focuses on the dissemination of local news, events, and initiatives that encourage community participation and awareness.
Global Travel Experiences	This topic encompasses the exploration and enjoyment of diverse travel destinations and cultural experiences worldwide, facilitated by convenient booking and travel arrangements.
Manufacturing Innovations	This topic encompasses the latest advancements and innovations in manufacturing processes and product design across diverse industries, emphasizing quality, efficiency, and technological improvements.
Film and TV Entertainment	This topic encompasses the latest developments, releases, and events in the film and television industry, particularly focusing on superhero and action genres, film festivals, and popular franchises.
Political Ideological Tensions	The topic encompasses the ongoing political and ideological conflicts in the United States, emphasizing leadership, civil unrest, religious freedom, and conservative principles.
Home and Property Maintenance	This topic encompasses a range of services aimed at maintaining and improving residential and commercial properties, ensuring they are clean, functional, and aesthetically pleasing.

Continued on next page

Table 2 – continued from previous page

Taxonomy	Description
Personal Reflections and Musings	This topic involves sharing personal anecdotes, contemplations, and humorous insights on everyday life and broader philosophical questions, often in a casual and engaging narrative style.
Inclusive and Adaptive Education	This topic focuses on educational strategies and programs designed to promote inclusivity, accessibility, and adaptability to meet the diverse needs of students and educators in evolving academic and career landscapes.
Website User Interaction	This topic covers the various aspects of user engagement with websites, including privacy settings, account management, and customer support services.
Science-Backed Natural Health Solutions	This topic focuses on the integration of scientific research and natural ingredients to promote health and wellness, offering solutions for skincare, energy enhancement, and weight management.
Personal Financial Management	This topic encompasses strategies and resources for effectively managing personal finances in diverse situations, including moving, property division, home improvement, and budgeting.
Community and Local Governance	The topic encompasses community resilience, local government initiatives, and administrative challenges within county-level governance.
Global Financial Markets and Investment Strategies	This topic encompasses the analysis of economic trends, investment strategies, and the impact of government policies on global financial markets.
Sports Events and Updates	This topic encompasses the latest developments, competitions, and strategic changes in various sports, providing insights into the dynamic world of sports management and events.
Technology-Driven Industry Automation	The cluster explores how cutting-edge technologies and automation are transforming industry practices, enhancing operational efficiency, and driving innovation across sectors.
Digital Marketing Strategies	This topic covers methods and tools for optimizing digital marketing to improve business visibility, audience engagement, and overall success.
Healthcare Challenges and Innovations	This topic encompasses the exploration of healthcare challenges, patient experiences, and innovative approaches to treatment and care delivery.
Online Slot Gaming	Online Slot Gaming refers to the digital version of traditional slot machines, offering players an engaging and convenient way to experience casino excitement with diverse themes and features.
Consumer Product Design and Retail	This topic encompasses the design, quality, and retail aspects of various consumer products, focusing on unique craftsmanship and customer shopping experiences.
Adult Entertainment Industry	This topic encompasses the production, distribution, and consumption of adult content, including live performances, online platforms, and the economic aspects of the adult entertainment sector.
Culinary Exploration and Sustainability	This topic encompasses the art of cooking, the enjoyment of diverse flavors, and the significance of sustainable food practices.
Geopolitical Conflict and Human Rights Violations	This topic encompasses the examination of violence, military actions, and human rights abuses in conflict zones, highlighting the systematic nature of these issues and their impact on civilians and freedom of expression.

B.2.2. PROMPT FOR TAXONOMY GENERATION

Prompt for Taxonomy Generation

You are an expert data taxonomist.

I will provide you with $\{len(indices)\}$ documents that belong to the same semantic cluster.

Your task is to:

1. Summarize the common theme and content of these documents in 2-3 sentences.
2. Based on the summary, assign a single, concise, and high-quality 'Topic Label' (2-5 words) that best describes this cluster.
3. Describe the topic in a sentence.

Documents:

$\{docs_content\}$

Please strictly follow the output format:

Summary: summary content

Topic: topic label

Description: topic description

B.3. Quantitative Coherence and GIS Ablations

To complement the qualitative taxonomy visualization in Figure 3, we evaluate semantic consistency using automated topic-coherence metrics. For each categorization strategy, we extract the top-15 TF-IDF words per cluster and compute Normalized Pointwise Mutual Information (NPMI) and the C_V score over a large sampled corpus. As shown in Table 3, GEM achieves topic coherence on par with the LLM-annotated WebOrganizer Topic taxonomy while retaining a fully unsupervised, model-native partitioning process.

Table 3. Automated topic-coherence evaluation across taxonomies. Higher is better.

Taxonomy Strategy	NPMI \uparrow	C_V Score \uparrow
WebOrganizer Format	-0.1219	0.4341
WebOrganizer Topic	-0.0700	0.4943
GEM (Ours)	<u>-0.0728</u>	<u>0.4928</u>

We further ablate the representative-sample selection rule used for taxonomy generation. For each cluster, we select five samples under each heuristic, prompt an LLM to generate the topic description, and then use the description as a prompt for labeling a held-out set of 720 samples. Table 4 shows that GIS yields the highest labeling accuracy, indicating that combining assignment certainty, directional coherence, and local support produces more semantically robust prototypes than simpler alternatives.

Table 4. Ablation study on prototype selection heuristics for taxonomy generation.

Selection Method	Selection Criteria	Accuracy (%)
Random Sampling	Uniform random	80.41
Confidence-only	Maximize $\log \gamma_{ik}$	80.83
Center-only	Maximize $\kappa_k \mu_k^\top x_i$	81.67
GIS (Ours)	Eq. (21)	84.17

B.4. Qualitative Comparison with K-Means

We also inspect representative cases where GEM and K-Means produce different cluster assignments. In one case, documents about configuring a vanity URL shortener and open-source conference sprints were separated by K-Means into

surface-level website-interaction and politics-related clusters, whereas GEM placed both into a coherent technology and software-development cluster. In another case, a technical endoscopic-surgery abstract and a sunscreen news article shared generic medical vocabulary and were grouped together by K-Means; GEM separated them into healthcare-innovation and natural-health clusters, respectively. These cases illustrate that GEM’s directional probabilistic modeling can reduce both unnatural fragmentation and inappropriate grouping caused by superficial lexical overlap.

C. Details of Scalable Deployment

To scale GEM to trillion-token datasets, we employ a two-phase Teacher-Student approach. This ensures that the high-quality geometric partitions discovered by GEM can be applied to web-scale data without incurring the computational cost of the EM algorithm on the entire corpus.

Phase 1: Clustering and GIS-Guided Pseudo-Labeling. We first apply GEM to a randomly sampled subset $\mathcal{X}_{\text{seed}} \subset \mathcal{X}$ to obtain the converged directional parameters $\Theta^* = \{(\mu_k, \kappa_k)\}_{k=1}^K$. Using these learned directions as anchors, we retrieve candidate samples from the larger unlabeled pool. To mitigate topic-frequency skew and ensure the student model learns from semantically representative prototypes, we enforce cluster-wise balanced sampling governed by the GIS score (defined in Eq. 21). Specifically, for each cluster C_k , we select the top- M samples ranked by their GIS values, yielding a balanced pseudo-labeled dataset:

$$\mathcal{D}_{\text{train}} = \bigcup_{k=1}^K \{(w_i, y_i = k) \mid x_i \in \text{Top-}M(\text{GIS}(x \mid \Theta^*))\}, \quad (25)$$

where w_i denotes the raw text corresponding to embedding x_i . By prioritizing samples with high GIS, we ensure that the distilled dataset consists of candidates with high model certainty, geometric centrality, and dense local manifolds, effectively filtering out noise and ambiguous samples near decision boundaries.

Phase 2: Lightweight Student Classifier Distillation. We train a lightweight text-space classifier $f_\phi : w \mapsto \Delta^{K-1}$ to approximate the GEM-induced partition function. In our implementation, we adopt **FastText** (Joulin et al., 2017) due to its constant-time inference complexity with respect to corpus size and its strong inductive bias toward linear, directionally separable decision boundaries, which aligns well with the directional nature of vMF distributions.

The student model is optimized via cross-entropy loss on the curated dataset $\mathcal{D}_{\text{train}}$:

$$\mathcal{L}_{\text{student}}(\phi) = - \sum_{(w,y) \in \mathcal{D}_{\text{train}}} \log P_{\text{FastText}}(y \mid w; \phi). \quad (26)$$

Once trained, this classifier is deployed to process the full-scale pre-training corpus, assigning a probability distribution over the K latent topics to every document.

D. Pre-training Details

We conduct pre-training experiments using the Llama Factory framework on a high-performance compute node equipped with $8 \times$ NVIDIA GeForce RTX 5090 GPUs. The models are optimized using the AdamW optimizer with a peak learning rate of 4×10^{-4} , supplemented by a linear warmup phase of 2,000 steps and a subsequent cosine annealing schedule. To ensure training stability and throughput, we employ a global batch size of 256, achieved through a configuration of 8 GPUs, a micro-batch size of 16, and 2 gradient accumulation steps. Regularization is applied via a weight decay of 0.1, and the maximum sequence length is constrained to a 2,048-token cutoff. All comparative experiments maintain these standardized hyperparameters to isolate the empirical impact of the GEM-induced taxonomy on downstream performance.

E. Details of Implementation for Data Classification Strategies

To operationalize the semantic partitions at scale, we train a lightweight fastText (Joulin et al., 2017) classifier to approximate the clustering assignment. For a rigorous comparison, we curated balanced datasets for both the K -Means baseline and the proposed GEM framework by randomly sampling 5,000 documents per cluster, which were subsequently partitioned into training, validation, and test sets following an 8:1:1 ratio. For Spherical K -Means, all embeddings are ℓ_2 -normalized and centroids are renormalized after each update, yielding hard assignments under cosine similarity with the same K as the corresponding GEM run. While the classifier trained on K -Means annotations achieved a test accuracy of 72.92%,

the model distilled from GEM partitions attained a superior accuracy of 75.13%. This performance advantage indicates that the partitions generated by GEM on the Riemannian manifold possess higher intrinsic semantic consistency and clearer separation boundaries compared to Euclidean clusters, thereby reducing label noise and facilitating more robust generalization in the student classifier.

F. Details of Implementation for Data Mixing Strategies

In this section, we provide the specific implementation details for the data mixing strategies compared in our main experiments.

Perf. Perf utilizes a sensitivity-driven heuristic inspired by task-oriented sampling to identify and amplify high-value domains. This strategy is similar to PerfRe introduced by (Peng et al., 2025). The process begins with a sensitivity profiling phase, where we measure the contribution of each domain by individually upsampling it by 30% in temporary experimental mixtures and evaluating the resulting proxy model on downstream tasks. Guided by these performance rankings, we construct the final training distribution through a stratified upsampling scheme: the top two domains are upsampled by 40%, the third and fourth ranked domains are upsampled by 20%, and the remaining data budget is distributed uniformly across all other categories.

REGMIX. REGMIX formulates data-mixture selection as a regression problem. It first samples a diverse set of candidate mixtures (e.g., from a Dirichlet distribution anchored to the base token distribution) and trains proxy models under these mixtures to obtain a scalar target signal for each candidate (typically a validation-domain loss). REGMIX then fits a regressor from mixture weights to the target signal, and uses large-scale mixture simulation with fast regression inference to rank candidates and derive a robust final training distribution (e.g., by selecting or averaging the top-ranked predicted mixtures). In our instantiation, we train **256** proxy models with **1M** parameters, each for **1B** tokens.

DoReMi. DoReMi formulates data-mixture learning as a distributionally robust (minimax) reweighting problem. It first trains a *reference* model, and then trains a *proxy* model while *online* updating domain weights based on per-domain *excess loss* relative to the reference model, typically using exponentiated-gradient-style updates with smoothing. The resulting (time-averaged) weights are then used as a fixed data mixture for training the final model. In our setting, both the reference and proxy models have **120M** parameters and are each trained for **10B** tokens.

Table 5. Results on Science QA benchmarks.

Model Variation	ARC-C	ARC-E	SciQ	OBQA	Avg
Under DoReMi					
K-Means	26.62	49.30	25.60	27.20	32.18
TOS	25.34	50.00	27.00	27.60	32.49
WebOrganizer Topic	25.43	50.20	29.10	34.00	34.68
WebOrganizer Format	25.94	50.10	28.50	33.20	34.44
GEM (Ours)	26.37	50.60	28.80	33.40	34.79
Under Perf					
K-Means	24.91	48.70	25.10	31.20	32.48
TOS	25.94	48.80	28.00	27.40	32.54
WebOrganizer Topic	25.68	50.10	29.80	34.60	35.05
WebOrganizer Format	25.43	50.80	29.60	34.40	35.06
GEM (Ours)	25.94	51.90	30.00	36.00	35.96
Under RegMix					
K-Means	26.62	47.90	25.00	27.00	31.63
TOS	26.02	48.30	26.00	28.40	32.18
WebOrganizer Topic	26.79	49.60	26.20	33.00	33.90
WebOrganizer Format	25.77	49.80	26.90	34.00	34.12
GEM (Ours)	26.28	50.20	26.40	33.40	34.07

Table 6. Results on Commonsense Reasoning benchmarks.

Model Variation	CSQA	Hella	PIQA	Avg
Under DoReMi				
K-Means	19.74	26.20	56.70	34.21
TOS	21.38	24.80	56.70	34.29
WebOrganizer Topic	19.98	34.40	60.40	38.26
WebOrganizer Format	20.80	34.80	60.60	38.73
GEM (Ours)	20.97	37.40	61.50	39.96
Under Perf				
K-Means	22.03	29.10	54.20	35.11
TOS	21.62	28.80	53.10	34.51
WebOrganizer Topic	20.80	35.20	63.20	39.73
WebOrganizer Format	20.88	35.50	62.80	39.73
GEM (Ours)	20.88	37.60	62.80	40.43
Under RegMix				
K-Means	20.07	26.30	58.20	34.86
TOS	22.36	25.00	55.70	34.35
WebOrganizer Topic	21.38	25.60	54.50	33.83
WebOrganizer Format	21.21	25.30	55.30	33.94
GEM (Ours)	21.21	27.50	57.20	35.30

Table 7. Results on Logic & Linguistics benchmarks.

Model Variation	Wino	COPA	Avg
Under DoReMi			
K-Means	48.86	58.00	53.43
TOS	49.96	58.00	53.98
WebOrganizer Topic	51.70	59.00	55.35
WebOrganizer Format	51.38	59.00	55.19
GEM (Ours)	51.22	63.00	57.11
Under Perf			
K-Means	50.04	61.00	55.52
TOS	49.57	57.00	53.29
WebOrganizer Topic	49.80	66.00	57.90
WebOrganizer Format	48.93	67.00	57.97
GEM (Ours)	49.96	66.00	57.98
Under RegMix			
K-Means	52.33	59.00	55.67
TOS	49.80	55.00	52.40
WebOrganizer Topic	50.99	54.00	52.50
WebOrganizer Format	50.51	58.00	54.26
GEM (Ours)	51.93	58.00	54.97

G. Details of implementation for Data Mixing Predictability

We sample **256** mixture vectors $\{w_j\}_{j=1}^{256}$ from the simplex and, following the standard RegMix protocol, train one **proxy model** (1M parameters) per mixture to obtain the corresponding validation loss $\{L_j\}_{j=1}^{256}$. We then fit the RegMix regression model on pairs (w_j, L_j) using an **80/20 split** over mixture points (205 for training, 51 for testing). To assess predictability on the held-out mixtures, we compute the **Spearman rank correlation** (ρ) between the ground-truth losses and the RegMix-predicted losses on the test mixtures. Higher ρ indicates that the regression model preserves the ordering of losses induced by mixture weights, suggesting that the taxonomy yields less noisy, less collinear, and more disentangled mixing factors.

H. Additional Results

H.1. Full Downstream Results

We report detailed results on all nine benchmarks, categorized into three dimensions: **Science QA** (Table 5), **Commonsense Reasoning** (Table 6), and **Logic & Linguistics** (Table 7).

H.2. Pilot Study on Downscaled Proxies.

To efficiently validate our training configuration and investigate the early-stage capability acquisition, we conduct a controlled pilot study using a downscaled model setup across a range of 5B to 25B tokens. As illustrated in Figure 8, the model exhibits a consistent and monotonic improvement in *Average* performance (from 41.05% to 42.12%), confirming the stability of our optimization trajectory at a reduced scale. A granular analysis reveals diverging learning dynamics across different task categories: while *Science QA* and *Commonsense Reasoning* show steady gains—suggesting a continuous integration of world knowledge—the performance in *Logic & Linguistics* plateaus relatively early after 5B tokens. This observation indicates that fundamental linguistic structures are captured during the initial phase of pre-training, whereas complex reasoning benefits more significantly from extended token exposure.

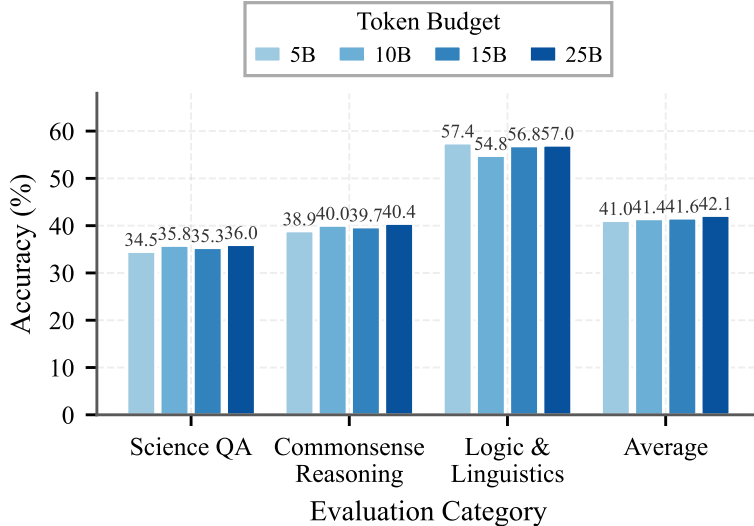


Figure 8. **Pilot Study on Downscaled Proxies.** The model exhibits a consistent and monotonic improvement in *Average* performance (from 41.05% to 42.12%), confirming the stability of our optimization trajectory at a reduced scale.

I. Additional Robustness and Sensitivity Analyses

I.1. Robustness to AI-Generated Content Contamination

As web corpora increasingly contain AI-generated content (AIGC), data curation methods must remain robust to synthetic regions that may be unusually dense in embedding space. Such density can amplify the cluster-collapse behavior of hard Euclidean clustering, pulling otherwise distinct human-written documents into AIGC-dominated clusters. GEM mitigates this failure mode through the mixing-balance regularizer on the empirical mass $\pi(\Gamma)$, which penalizes artificially dominant regions while preserving angular semantic structure. In our corpus, the RefinedWeb-style filtering pipeline removes most low-quality or synthetic spam, and a Binoculars-based screening (Hans et al., 2024) estimates the proportion of likely AI-generated content to be below 0.5%. As an additional stress test, mixing natural web data with Cosmopedia, a synthetic web-style corpus (Ben Allal et al., 2024), caused K-Means to assign 37.5% of synthetic data to two massive clusters, whereas GEM maintained balanced semantic partitions without global collapse.

I.2. Sensitivity to the Balance Regularizer

We study the contribution of the mixing-balance regularizer by varying λ while keeping the remaining experimental setting fixed. Since the E-step assignment logits are dominated by vMF log-likelihood differences whose scale is governed by learned concentrations around $\kappa \approx 900$, we set $\lambda = 5000$ as the default value in the main experiments to align the regularizer with this logit scale. Table 8 shows that vanilla vMF clustering without the balance term already provides a strong hyperspherical baseline, while the full GEM objective achieves the best average performance. The results are also stable across a broad range of nonzero λ values, suggesting that GEM does not depend on a finely tuned regularization coefficient.

Table 8. Ablation study isolating the contribution and sensitivity of the regularizer coefficient λ under GEM + Perf.

Regularizer Coefficient	Science QA	Commonsense	Logic & Linguistics	Average
$\lambda = 0$ (Vanilla vMF)	34.55	40.21	56.27	43.68
$\lambda = 1000$	35.19	40.21	55.70	43.70
$\lambda = 5000$ (Adopted)	35.96	40.43	57.98	44.79
$\lambda = 10000$	35.81	39.58	56.68	44.05

I.3. Sensitivity to Seed Corpus Size

The teacher phase runs GEM on a representative seed corpus $\mathcal{X}_{\text{seed}}$ before distilling the learned partitions into the student classifier. To evaluate the data efficiency of this stage, we vary the seed corpus from 1B to 10B tokens. As shown in Table 9, GEM already induces a competitive taxonomy with 1B seed tokens, improves at the 3B-token default, and yields only marginal additional gains at 10B tokens. This supports the use of a moderate seed corpus for efficient web-scale deployment.

Table 9. Sensitivity analysis on the size of the seed corpus $\mathcal{X}_{\text{seed}}$ under GEM + Perf.

Seed Corpus Size	Science QA	Commonsense	Logic & Linguistics	Average
1B Tokens	35.35	39.77	57.89	44.37
3B Tokens (Default)	35.96	40.42	57.98	44.79
10B Tokens	35.60	40.12	58.80	44.86

I.4. Learned vMF Concentrations

To characterize the geometry learned by GEM, we report summary statistics of the vMF concentration parameter κ across different cluster granularities. Larger κ values correspond to tighter directional concentration. The consistently high values in Table 10 indicate that the learned clusters are compact on the hypersphere, providing empirical support for modeling the embedding space with directional distributions rather than ambient Euclidean distances alone.

Table 10. Statistics of the learned vMF concentration parameter κ across different numbers of clusters.

Number of Clusters	Mean	Median	Min	Max	Std. Dev.
$K = 12$	881.19	884.61	854.07	904.58	14.49
$K = 24$	912.93	910.19	814.34	952.59	32.26
$K = 36$	931.79	934.83	822.89	965.92	28.48
$K = 48$	942.66	945.84	830.18	978.69	30.10

J. Pseudocode of GEM

Algorithm 1 summarizes the computational pipeline of GEM, which maximizes the entropy-regularized variational objective in Eq. (3) via an MM-based (minorize–maximize) alternating optimization scheme. The algorithm starts with spherical initialization, then iteratively performs (i) an *E-step* that increases the MM surrogate $\tilde{\mathcal{F}}_t$ in Eq. (10) (hence guaranteeing monotonic ascent of \mathcal{F} ; Theorem A.1), and (ii) an *M-step* that updates vMF parameters in closed form. After convergence, GEM optionally selects representative samples using Geometric Influence Scores (GIS) for taxonomy generation, and distills the learned partition into a lightweight student classifier for web-scale deployment (details in Appendix).

Algorithm 1 GEM: Geometric Entropy Mixing via MM-Based vMF Clustering

Require: Embeddings $\mathcal{X} = \{x_i\}_{i=1}^N \subset \mathcal{S}^{d-1}$, number of clusters K , balance strength $\lambda > 0$, maximum iterations T_{\max} , tolerance $\varepsilon_{\text{stop}} > 0$, small constant $\varepsilon > 0$ for numerical stability, optional: GIS neighborhood size k_{nn} and top- M representatives per cluster.

Ensure: Soft assignments $\Gamma = \{\gamma_{ik}\}$, parameters $\Theta = \{(\mu_k, \kappa_k)\}_{k=1}^K$, (optional) representative sets $\{\mathcal{S}_k\}_{k=1}^K$.

```

1: // Initialization
2: Initialize  $\{\mu_k^{(0)}\}_{k=1}^K$  by spherical  $k$ -means on  $\mathcal{X}$ .
3: Initialize  $\kappa_k^{(0)} \leftarrow \kappa_{\text{init}} \geq 0$  for all  $k$ .
4: Initialize responsibilities  $\gamma_{ik}^{(0)} \leftarrow \frac{1}{K}$  for all  $i, k$ .
5: Set fixed generative prior  $\alpha_k \leftarrow \frac{1}{K}$  for all  $k$ .
6: for  $t = 0$  to  $T_{\max} - 1$  do
7:   Compute empirical masses  $\pi_k^{(t)} \leftarrow \frac{1}{N} \sum_{i=1}^N \gamma_{ik}^{(t)}$  for all  $k$ .
8:   Set  $\boldsymbol{\pi}^{(t)} \leftarrow (\pi_1^{(t)}, \dots, \pi_K^{(t)})$  and  $\mathbf{u} \leftarrow \frac{1}{K} \mathbf{1}$ .
9:   Compute  $\nabla R(\boldsymbol{\pi}^{(t)}) \leftarrow -\lambda(\boldsymbol{\pi}^{(t)} - \mathbf{u})$  {Eq. (7)}
10:  — E-step (MM): increase the surrogate  $\tilde{\mathcal{F}}_t$  —
11:  Define  $\tilde{\mathcal{F}}_t(\Gamma)$  by Eq. (10) (using  $\Theta^{(t)}$  and  $\boldsymbol{\pi}^{(t)}$ ).
12:  Obtain  $\Gamma^{(t+1)}$  such that  $\tilde{\mathcal{F}}_t(\Gamma^{(t+1)}) \geq \tilde{\mathcal{F}}_t(\Gamma^{(t)})$  {Eq. (17)}
13:   Implementation note: maximize  $\tilde{\mathcal{F}}_t$  over  $\{\gamma_i \in \Delta^{K-1}\}$  using a few steps of projected/mirror ascent; any update satisfying the inequality is valid.
14:  — M-step: closed-form vMF updates —
15:  for  $k = 1$  to  $K$  do
16:     $r_k^{(t+1)} \leftarrow \sum_{i=1}^N \gamma_{ik}^{(t+1)} x_i$ .
17:     $N_k^{(t+1)} \leftarrow \sum_{i=1}^N \gamma_{ik}^{(t+1)}$ .
18:     $\mu_k^{(t+1)} \leftarrow \frac{r_k^{(t+1)}}{\|r_k^{(t+1)}\|_{2+\varepsilon}}$  {Eq. (14)}
19:     $\bar{R}_k^{(t+1)} \leftarrow \frac{\|r_k^{(t+1)}\|_2}{N_k^{(t+1)} + \varepsilon}$ .
20:     $\kappa_k^{(t+1)} \leftarrow \frac{\bar{R}_k^{(t+1)} d - (\bar{R}_k^{(t+1)})^3}{1 - (\bar{R}_k^{(t+1)})^2 + \varepsilon}$  {Eq. (16)}
21:  end for
22:  — Stopping criterion —
23:  Compute  $\Delta \leftarrow |\mathcal{F}(\Theta^{(t+1)}, \Gamma^{(t+1)}) - \mathcal{F}(\Theta^{(t)}, \Gamma^{(t)})|$  {Eq. (3)}
24:  if  $\Delta \leq \varepsilon_{\text{stop}}$  then
25:    break
26:  end if
27: end for
28: // Optional: GIS-based representative selection for interpretability (Appendix B)
29: if GIS sampling is enabled then
30:   for  $k = 1$  to  $K$  do
31:     $\mathcal{I}_k \leftarrow \{i : \arg \max_j \gamma_{ij} = k\}$  {hard assignment for sampling only}
32:    for each  $i \in \mathcal{I}_k$  do
33:      Compute a GIS score  $\text{GIS}(x_i; k)$  using  $\gamma_{ik}, \mu_k, \kappa_k$ , and  $\rho_{\text{local}}(x_i)$  (see Appendix B).
34:    end for
35:     $\mathcal{S}_k \leftarrow$  top- $M$  samples in  $\mathcal{I}_k$  with the largest GIS scores.
36:   end for
37: end if
38: return  $\Gamma^{(t+1)}, \Theta^{(t+1)}$ , and (if enabled)  $\{\mathcal{S}_k\}_{k=1}^K$ .
    
```